

May 30, 2023

MIT-CTP 5499

Renormalons in the energy-energy correlator

Stella T. Schindler,^a Iain W. Stewart,^a and Zhiquan Sun^a

^a*Center for Theoretical Physics, Massachusetts Institute of Technology
77 Massachusetts Ave., Cambridge, MA 02139, USA*

E-mail: stellas@mit.edu, iains@mit.edu, zqsun@mit.edu

ABSTRACT: The energy-energy correlator (EEC) is an observable of wide interest for collider physics and Standard Model measurements, due to both its simple theoretical description in terms of the energy-momentum tensor and its novel features for experimental studies. Significant progress has been made in both applications and higher-order perturbative predictions for the EEC. Here, we analyze the nature of the asymptotic perturbative series for the EEC by determining its analytic form in Borel space under the bubble-sum approximation. This result provides information on the leading and subleading nonperturbative power corrections through renormalon poles. We improve the perturbative convergence of the $\overline{\text{MS}}$ series for the EEC by removing its leading renormalon using an R scheme, which is independent of the bubble-sum approximation. Using the leading R-scheme power correction determined by fits to thrust, we find good agreement with EEC OPAL data already at $\mathcal{O}(\alpha_s^2)$.

Contents

1	Introduction	1
1.1	Borel summation and renormalons	3
2	EEC renormalons	5
2.1	Leading order	5
2.2	Bubble diagram calculation	6
2.2.1	Modified gluon propagator probe	7
2.2.2	Borel-space result	9
2.3	Renormalons in the EEC	10
2.3.1	Renormalon series in $\overline{\text{MS}}$	12
3	Mitigating renormalon effects with an R scheme	13
3.1	EEC in the R scheme	13
3.2	R scheme with resummation	15
3.3	Perturbative convergence	15
3.4	Nonperturbative corrections and hadron masses	16
3.5	Comparison to experimental data	18
4	Concluding remarks	19

1 Introduction

A central challenge of high-energy physics is to develop observables that are easily accessible experimentally, have a clean and clear connection to dynamics of interest in the underlying physical theory, and can be computed theoretically at high precision. An important observable for quantum chromodynamics that currently satisfies the first two criteria is the energy-energy correlator (EEC), an infrared and collinear (IRC) safe event shape that characterizes the angular distribution of particles produced in e^+e^- collisions [1, 2],

$$\frac{d\Sigma}{d\cos\chi} = \sum_{i,j} \int d\sigma \frac{E_i E_j}{Q^2} \delta(\cos\chi - \cos\theta_{ij}). \quad (1.1)$$

The EEC has many useful generalizations, including the transverse EEC (TEEC) for hadron-hadron collisions [3], multi-point energy correlators [4], as well as EEC and TEEC observables for electron-hadron colliders [5, 6]; it is also related to energy correlation functions for jets [7–9]. Nonperturbative contributions to energy correlators are expected to be small, making them compelling candidates for studying strong interactions [10], whether through extracting the QCD coupling constant [11, 12], investigating transverse momentum distributions [5, 6], or probing factorization violation [13]. These observables have been measured at LEP and the LHC at CERN [14–19], SLD at SLAC [20], and are a target of

the planned Electron-Ion Collider at Brookhaven [21]. To interpret experimental data, it is important to have corresponding high-precision theoretical predictions.

The EEC was first studied at leading order in the 1970s [2], instigating a decade of work producing numerical predictions at next-to-leading order (NLO) [22–30]. It took two further decades to achieve the first numerical results at next-to-next-to-leading order (NNLO) [31, 32] and analytic results at NLO [33]. Higher-order perturbative results for the EEC exist only for certain cases: in the so-called collinear limit at next-to-next-to-leading logarithms (NNLL) [34–36], in the back-to-back limit at $N^3\text{LO}$, $N^3\text{LL}'$ and $N^4\text{LL}$ [32, 37–42], as well as for $\mathcal{N} = 4$ supersymmetric Yang-Mills theory both at leading power at NNLO and at subleading power only in the back-to-back limit [43–47].

There has been much less recent work on nonperturbative power corrections for the EEC. Ref. [48] pointed out that the EEC has Λ_{QCD}/Q power corrections for all values of the angular variable χ , in contrast to event shapes for which such power corrections appear in the dijet limit. Ref. [48] also carried out a renormalon calculation for a weighted integral over the EEC, finding a result in agreement with the presence of $1/Q$ power corrections. Ref. [49] initiated the use of operator methods to study EEC power corrections, and argued that the leading corrections take the form

$$\frac{1}{\sigma_0} \frac{d\Sigma}{d\cos\chi} = \frac{1}{\sigma_0} \frac{d\hat{\Sigma}}{d\cos\chi} + \frac{2}{\sin^3\chi} \frac{\bar{\Omega}_1}{Q}, \quad (1.2)$$

with $\bar{\Omega}_1 \sim \Lambda_{\text{QCD}}$. Here $\bar{\Omega}_1 = \lambda_1/2$ in the notation of ref. [49, 50]. Note that relative to [49, 50], we multiply by 2π for the azimuthal angular integral and include an additional combinatoric factor of 2, since either of the energies E_i or E_j can become nonperturbative. Ref. [51] reached this same conclusion in the dispersive model for power corrections with the same factors of 2 shown in eq. (1.2), and also considered perturbative corrections to the power correction coefficient. The universality of the power correction is not violated by gluon splitting [52], an effect known as the Milan factor [53]. The earliest prediction for the $1/\sin^3\chi$ behavior of EEC power corrections was in the fragmentation model of ref. [2]. Our $\bar{\Omega}_1$ notation follows ref. [54], where a value of $\bar{\Omega}_1$ for thrust was determined by a fit to data. Using massless kinematics, the parameter $\bar{\Omega}_1$ appearing for the EEC is the same as the one appearing in the dijet limit of thrust and other e^+e^- event shapes [49, 50, 55]; however, this universality can be spoiled by $\mathcal{O}(1)$ hadron mass corrections, which depend on the method used to reconstruct particle energies and momenta [56, 57].

Interestingly, to our knowledge, a direct bubble-sum renormalon calculation of the χ -dependence of the $1/Q$ power correction to the EEC in Borel space has not yet been carried out, so we do so here. Our expectation is that the leading Borel-space renormalon will agree with the $1/\sin^3\chi$ in eq. (1.2); however, the renormalon analysis method relies on completely different approximations than the operator-based approach, and thus provides an independent nontrivial confirmation. The Borel-space result also gives access to higher-order renormalons. We find that in the bubble-sum approximation, there is no renormalon corresponding to an $\mathcal{O}(1/Q^2)$ power correction. Additionally, our calculations provide input to assess the convergence of the $\overline{\text{MS}}$ -scheme perturbative expansion for the EEC, which is known to be asymptotic. At $\mathcal{O}(\alpha_s^2)$, we observe that the large- β_0 approximation provides a

reasonable approximation to the full result. From fig. 1 of ref. [32] at $\mathcal{O}(\alpha_s^3)$, we note that the EEC seems to exhibit slow perturbative convergence for some values of χ . This is also true for the $z \rightarrow 0$ fixed-order and resummed results in ref. [34].

We present a scheme change from $\overline{\text{MS}}$ to an R scheme [54, 58, 59], which removes the leading renormalon from both the perturbative EEC series and its leading power correction. This scheme change yields improved convergence for the perturbative EEC series. Using the universality between the thrust and EEC $\bar{\Omega}_1$ parameters, we show that our R scheme results are already consistent at $\mathcal{O}(\alpha_s^2)$ with EEC data from the OPAL experiment at LEP [60].

The outline of this paper is as follows. Section 1.1 provides a brief overview of asymptotic series and the types of divergences that they may exhibit, including renormalons. In section 2, we utilize the bubble chain formalism for probing renormalons from the infrared structure of final-state gluons to calculate a Borel space result for the EEC, and demonstrate that its leading renormalon is consistent with the $1/Q$ power correction in eq. (1.2), while a renormalon corresponding to the $1/Q^2$ power correction is absent. In section 3, we show how to remove the $u = 1/2$ renormalon from the $\overline{\text{MS}}$ perturbative series using an R scheme, and demonstrate that this improves both perturbative convergence and agreement with experimental data. We make concluding remarks in section 4.

1.1 Borel summation and renormalons

Perturbative expansions of observables in QFT are generally asymptotic [61]: even if their first few terms appear to converge, at some order of expansion, the coefficients begin to rapidly grow. Divergences should not be viewed as a fundamental sickness of a theory; rather, asymptotic series encode all-orders nonperturbative information [62–66]. Nonetheless, extracting useful information from such a series is nontrivial; there are many different types of divergences, each of which must be handled in different ways.

Perhaps the most conspicuous source of divergence in QFT is factorial growth in the number of Feynman diagrams at high orders, which may lead to corresponding growth of the series [67–70]. The technique of Borel summation is often sufficient to overcome such growth. First, we take a Borel transform of an observable $f(\alpha_s) \rightarrow F(u)$, which for QCD is most often defined by:

$$f(\alpha_s) = \sum_{n=-1}^{\infty} c_n \alpha_s^{n+1} \rightarrow F(u) = c_{-1} \delta(u) + \sum_{n=0}^{\infty} \frac{c_n}{n!} \left(\frac{4\pi}{\beta_0} \right)^{n+1} u^n. \quad (1.3)$$

The factor of $4\pi/\beta_0$ provides a convenient normalization for the Borel variable u , where $\beta_0 = 11C_A/3 - 2n_f/3$ is the lowest order QCD β -function. Next, we compute the new, more rapidly convergent sum $F(u)$. Finally, we take an inverse Borel transform to recover the initial observable $f(\alpha_s)$:

$$f(\alpha_s) = \int_0^\infty du \exp \left[-u \frac{4\pi}{\beta_0 \alpha_s(\mu)} \right] F(u). \quad (1.4)$$

For more details of summation methods, see refs. [64, 71].

Borel summation techniques are powerful but not sufficient for every series. If an observable exhibits poles on the positive real axis in the complex- u Borel plane [72–74], the inverse Borel transform runs into a problem. In order to evaluate the integral in eq. (1.4), one must deform the integration contour above or below the real line to avoid the pole. Depending on where one chooses to deform the contour, the inverse Borel transform will yield different results. This leads to an ambiguity in the value of the perturbative series, the magnitude of which is given by the residue of the pole. Such poles are called infrared (IR) renormalons, which we hereafter refer to as simply renormalons (poles on the negative real axis are UV renormalons, which are not discussed here). Renormalons nearer to the origin create greater uncertainty in the value of a perturbative series, since the series coefficients grow as $\sim n! (2/p)^n$ for large n , given a pole at $u = p/2$.

Generally, one wishes to evaluate QCD observables theoretically at a level of precision comparable to experiment. Luckily, renormalon ambiguities in observables are unphysical: they cancel out between the perturbative series and nonperturbative matrix elements (or parameters of the field theory). We may view them as merely an artifact of not cleanly separating perturbative and nonperturbative contributions to an observable when carrying out a coupling expansion.¹

Renormalons originate in the IR region of momentum integrals in loop diagrams [64], and their behavior depends crucially on our choice of renormalization scheme; they appear in many schemes, such as the popular $\overline{\text{MS}}$ scheme. We may improve the convergence of a perturbative expansion by modifying our renormalization scheme choice for matrix elements (or parameters) in a manner that systematically removes these instabilities. This modification improves both perturbative behavior and the stability of the matrix element (or parameter) extraction. Examples of renormalons in QCD include the heavy-quark mass [89–93], the B^*-B mass splitting governed by the parameter λ_2 [58, 94], and hadronization parameters describing jet cross-sections [54, 90, 95–99]. In this paper, we obtain a Borel-space result for EEC renormalons, and then apply the method of ref. [58] to improve stability for the EEC.

¹The path integral formalism provides further intuition for divergent series in QFT. We may conceptualize perturbative effects as representing fluctuations about the vacuum, whereas nonperturbative effects arise from fluctuations about nontrivial saddle points. Some nonperturbative saddle points, such as instanton-anti-instanton pairs, are Borel summable [75, 76]. On the other hand, renormalons are connected to the more nuanced bions, or fractional instanton-anti-instanton pairs [65, 66, 77–83]. Developments from the rich and evolving field of hyper-asymptotics, resurgence theory, and trans-series [84–87] promise to provide further insight into nonperturbative effects in QFT as well as mathematical tools for handling asymptotic expansions unambiguously.

To construct a trans-series, one sums up a traditional perturbative series with a nonperturbative contribution, expressed as a complicated sum involving powers of exponential and logarithmic functions of the coupling. If one examines only a subset of terms in the trans-series, an imaginary ambiguity like a renormalon may arise. However, one expects [84] that a set of the so-called resurgence relations connecting the perturbative and nonperturbative sectors of the trans-series will cancel all ambiguities in the overall observable. This appears to be related to well-known phenomena in QCD where renormalon ambiguities are removed by using alternate renormalization schemes to define the perturbative and nonperturbative terms (see [64, 88] for reviews), which we explore later in this paper with an R scheme.

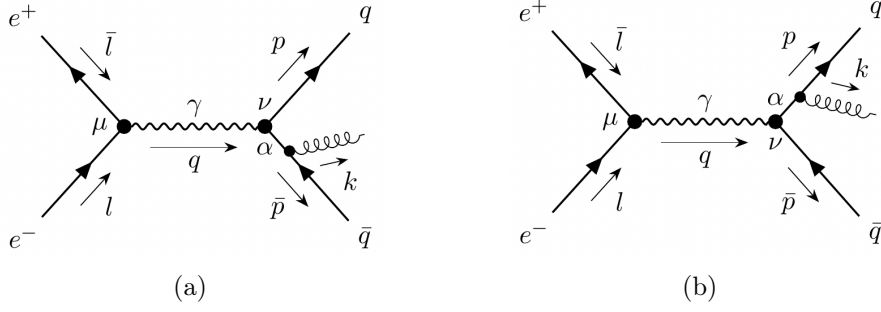


Figure 1: Leading-order diagrams for the energy-energy correlator in eq. (2.1).

2 EEC renormalons

The EEC describes how the energies of final-state hadrons in an e^+e^- collision are correlated, as a function of their angle χ relative to one another:

$$\frac{d\Sigma}{d\cos\chi} = \sum_{i,j} \int d\sigma_{e^+e^- \rightarrow ijX} \frac{E_i E_j}{Q^2} \delta(\cos\chi - \cos\theta_{ij}). \quad (2.1)$$

The right-hand side of eq. (2.1) is a weighted sum over differential cross-sections for all possible inclusive processes $e^+e^- \rightarrow ijX$ in which particles i and j are detected, with X representing the remaining (arbitrary) final states. We take the total invariant mass of the incoming e^+e^- to be Q^2 and work in the center-of-mass frame, where the measured final-state particles carry energy E_i and E_j and are separated by angle θ_{ij} .

2.1 Leading order

We begin by briefly reviewing the calculation of the EEC at leading order, as our renormalon studies directly build off of this result. At LO, the EEC is defined in terms of $e^+e^- \rightarrow q\bar{q}g$ Feynman diagrams shown in figure 1, and eq. (2.1) becomes

$$\frac{d\hat{\Sigma}}{dz} = \int \frac{d^3p}{2E} \frac{d^3\bar{p}}{2\bar{E}} \frac{d^3k}{2E_g} \frac{\delta^4(q - p - \bar{p} - k)}{(2\pi)^5} \sum_{i,j=q,\bar{q},g} \frac{E_i E_j}{Q^4} \delta(z - z_{ij}) \alpha_s(\mu) \langle |\mathcal{M}_0|^2 \rangle, \quad (2.2)$$

where we write the angular variable as $\cos\chi = 1 - 2z$ and $\cos\theta_{ij} = 1 - 2z_{ij}$. Here, p , \bar{p} , and k are the four-momenta of a final-state quark, anti-quark, and gluon, respectively, with corresponding energies E , \bar{E} , and E_g . The four-momentum of the virtual photon is q , with $Q^2 = q^2$. The initial-state leptons have four-momenta l and \bar{l} , and treating the leptons as unpolarized, we can average over both spins and leptonic angles relative to a given coordinate system. The spin-averaged LO matrix element $\langle |\mathcal{M}_0|^2 \rangle$ from summing figures 1a and 1b then evaluates to

$$\langle |\mathcal{M}_0|^2 \rangle = \sigma_0 \pi^2 2^9 C_F \frac{E^2 + \bar{E}^2}{(Q - 2E)(Q - 2\bar{E})}. \quad (2.3)$$

Here, the tree-level cross section is

$$\sigma_0 = \frac{4\pi\alpha^2}{Q^2} \sum_q e_q^2, \quad (2.4)$$

where e_q is the charge of a quark of flavor q . Plugging eq. (2.3) into eq. (2.2) and carrying out the phase space integrals, one finds the result for the EEC at $\mathcal{O}(\alpha_s)$:

$$\frac{1}{\sigma_0} \frac{d\hat{\Sigma}_{\text{LO}}}{dz} = \frac{\alpha_s C_F}{4\pi} \frac{3-2z}{z^5(1-z)} \left[3z(2-3z) + 2(3-6z+2z^2) \log(1-z) \right]. \quad (2.5)$$

Note that this cross-section scales as $1/z$ as $z \rightarrow 0$ and as $1/(1-z)$ as $z \rightarrow 1$ (modulo logarithms), and that this is the generic scaling expected for perturbative contributions to the EEC in these limits.

2.2 Bubble diagram calculation

Computing all possible radiative corrections to an observable and analyzing them for singularities is prohibitively involved. In QCD, it is conventional to instead examine the smaller set of so-called bubble diagrams to probe the existence of a renormalon. We define an n -bubble diagram by replacing the outgoing gluon in figure 1a and figure 1b by a chain of n fermion loops, shown in detail in figure 2. We must evaluate eq. (2.2) with \mathcal{M}_0 replaced by the sum \mathcal{M}_{bub} of all possible n -bubble diagrams, from $n = 0$ to ∞ :

$$\frac{d\hat{\Sigma}_{\text{bub}}}{dz} = \int \frac{d^3p}{2E} \frac{d^3\bar{p}}{2\bar{E}} \frac{d^3k}{2E_g} \frac{\delta^4(q - \sum p_i)}{(2\pi)^5} \sum_{i,j} \frac{E_i E_j}{Q^4} \delta(z - z_{ij}) \alpha_s(\mu) \langle |\mathcal{M}_{\text{bub}}|^2 \rangle, \quad (2.6)$$

where

$$i\sqrt{\alpha_s} \mathcal{M}_{\text{bub}} = \sum_{n=0}^{\infty} \left[\text{Diagram 1} + \text{Diagram 2} \right]. \quad (2.7)$$

Bubble diagrams comprise a gauge-invariant subset of all possible Feynman diagrams, which for n_f light quark flavors are proportional to n_f^k , with the highest possible power of k at each order in α_s . Thus, they serve as a convenient probe for the existence and severity of renormalon ambiguities [64]. Though the bubble diagram procedure is by nature imprecise, it nevertheless provides us sufficient information to both analyze and improve perturbative convergence, as well as better understand subleading power corrections.

It will be convenient to organize results at higher orders in perturbation theory in terms of color coefficients that involve $\{\beta_0, C_F, C_A, \dots\}$ rather than $\{n_f, C_F, C_A, \dots\}$. Here, $\beta_0 = 11C_A/3 - 2n_f/3$, and the ellipses denote terms beyond quadratic Casimirs. The basis with β_0 is more convenient here because terms with the maximum number of β_0 factors are known to numerically dominate perturbative series in many cases [100], while terms with C_F or C_A in place of a β_0 are numerically subleading. The renormalon bubble-chain calculation predicts precisely these leading- β_0 terms. Using the analytic results at $\mathcal{O}(\alpha_s^2)$ from ref. [33], one can confirm that for the EEC the β_0 terms numerically dominate, as we show in figure 3a.

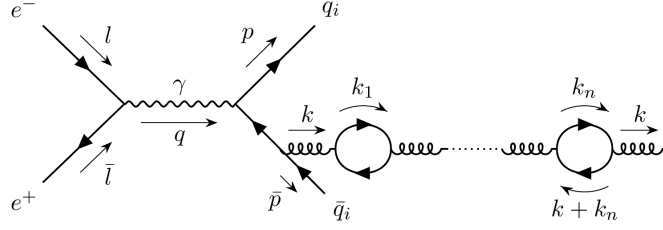


Figure 2: EEC bubble diagram, formed by replacing the external gluon in figure 1a with a chain of n fermion bubbles. Evaluating eq. (2.6) over the sum of all bubble diagrams allows us to probe for renormalon divergences in the EEC.

2.2.1 Modified gluon propagator probe

Our impetus to evaluate eq. (2.6) is that a bubble-sum-modified gluon propagator probes the infrared structure of the perturbative series, and thus can reveal renormalons. To make the gluon propagator explicit, we rewrite the gluon phase-space integral in eq. (2.6) as

$$\int \frac{d^3k}{2E_g} = 2 \int \frac{d^4k}{2\pi} \Theta(k^0) \text{Im} \left[\frac{1}{-k^2 - i0} \right]. \quad (2.8)$$

For expediency, we define $\Pi_g(k)$ as the gluon propagator times g^2 , i.e. $-(4\pi\alpha_s)iS^{\alpha\beta}/(k^2 + i0) = -4\pi iS^{\alpha\beta}\Pi_g(k)$. It is convenient to work in Lorentz gauge, so that the same transverse Lorentz index structure is present at tree level and in the presence of quark bubbles, in which case $S^{\alpha\beta} = (g^{\alpha\beta} - k^\alpha k^\beta/k^2)\delta^{ab}$. The effect of inserting bubbles into eq. (2.6) is

$$\langle |M_{\text{bub}}| \rangle^2 \Pi_g(k) = \langle |M_0| \rangle^2 \Pi_{\text{bub}}(k), \quad (2.9)$$

where Π_{bub} is the bubble-modified gluon propagator defined as

$$-4\pi i S^{\alpha\beta} \Pi_{\text{bub}}(k) = \sum_{n=0}^{\infty} \text{diagram with } n \text{ bubbles}, \quad (2.10)$$

where the dots on the ends give a factor of $g^2 = 4\pi\alpha_s$. Substituting eq. (2.9) into eq. (2.6),

$$\frac{d\hat{\Sigma}_{\text{bub}}}{dz} = 2 \int \frac{d^3p}{2E} \frac{d^3\bar{p}}{2\bar{E}} \frac{d^4k}{2\pi} \Theta(k^0) \sum_{i,j} \frac{E_i E_j}{Q^4} \delta(z - z_{ij}) \text{Im}[-\Pi_{\text{bub}}] \frac{\delta^4(q - \sum p_i)}{(2\pi)^5} \langle |\mathcal{M}_0|^2 \rangle. \quad (2.11)$$

We will make an approximation when evaluating eq. (2.11). Diagrammatically, the result for $\text{Im} \Pi_{\text{bub}}$ includes both terms with a cut gluon propagator and terms where a pair of quarks in a bubble are cut. While both of these cuts are included in our analysis, we allow the energy factors E_i and E_j to select only from the original q , \bar{q} , or a gluon with k^0 , and never from the individual quarks in the cut quark bubble. This has the virtue of significantly simplifying the calculation while still allowing the resulting modified gluon propagator to act as a probe of infrared dynamics.

Let us evaluate the series for Π_{bub} in eq. (2.10). The $n = 0$ term is $-4\pi i S^{\alpha\beta} \Pi_g$. The $n = 1$ renormalized result is well known:

$$\alpha \bullet \text{---} \xrightarrow{k} \bullet \text{---} \text{---} \text{---} \bullet \xrightarrow{k} \bullet \text{---} \beta = -\frac{2\alpha_s^2 n_f}{3} \frac{(-i S^{\alpha\beta})}{k^2 + i0} \ln \left(\frac{\mu^2 e^c}{-k^2 - i0} \right). \quad (2.12)$$

Again, we have included couplings and gluon propagators at either end. We use the modified minimal subtraction ($\overline{\text{MS}}$) renormalization scheme with parameter μ , and define $c = 5/3$. It is now straightforward to evaluate the bubble propagator sum in (2.10):

$$\Pi_{\text{bub}}(k) = \frac{1}{k^2 + i0} \frac{4\pi}{\beta_0} \sum_{n=0}^{\infty} \left(\frac{\alpha_s \beta_0}{4\pi} \right)^{n+1} \left[\ln \left(\frac{\mu^2 e^c}{-k^2 - i0} \right) \right]^n. \quad (2.13)$$

Here, we moved into the color coefficient basis $\{\beta_0, C_A, C_F, \dots\}$ by making the standard replacement $n_f \rightarrow -3\beta_0/2$. Next, we move eq. (2.13) into Borel space using eq. (1.3), taking $\alpha_s \beta_0/(4\pi)$ to the Borel variable u :

$$\Pi_{\text{bub}}(u) = \frac{-1}{(-k^2 - i0)^{1+u}} \frac{4\pi}{\beta_0} (\mu^2 e^c)^u, \quad (2.14)$$

We can now convert the bubble phase-space integral in eq. (2.11) back from four dimensions into a three-dimensional phase-space integral. When doing so, it is important to remember that the squared amplitude $\langle |\mathcal{M}_0|^2 \rangle$ and EEC weighting factor $E_i E_j$ are functions of energies, which we denote by $\mathcal{A}(k^0)$. For any $\mathcal{A}(k^0)$ we can carry out the transverse momentum integral to obtain²

$$\begin{aligned} 2 \int \frac{d^4 k}{2\pi} \Theta(k^0) \text{Im} \left[\frac{1}{(-k^2 - i0)^{1+u}} \right] \mathcal{A}(k^0) &= \int \frac{dk^+ dk^-}{2\pi} \Theta(k^0) \mathcal{A}(k^0) \text{Im} \left[\frac{d^2 k_{\perp}}{(\vec{k}_{\perp}^2 - k^+ k^- - i0)^{1+u}} \right] \\ &= \frac{\sin(\pi u)}{\pi u} 2\pi \int \frac{dk^+ dk^-}{4} \Theta(k^+) \Theta(k^-) (k^+ k^-)^{-u} \mathcal{A} \left(\frac{k^+ + k^-}{2} \right) \\ &= \frac{\sin(\pi u)}{\pi u} \int \frac{d^3 k}{2|\vec{k}|^{1+2u}} (\sin^2 \theta_k)^{-u} \mathcal{A}(|\vec{k}|). \end{aligned} \quad (2.15)$$

In the last line, we make the change of variable $k^{\pm} = |\vec{k}| \pm k^z$ to transform the result back into the form of a standard phase-space integral, and use $k^+ k^- = |\vec{k}_{\perp}|^2 = |\vec{k}|^2 \sin^2 \theta_k$. Here, θ_k is a polar angle defined relative to any fixed axis \hat{l} , a freedom we use later on. We now have all the ingredients we need for the bubble-approximated cross-section eq. (2.11).

²If we were to ignore $\mathcal{A}(k^0)$, it would be natural to carry out the k^0 integral to find the modified phase-space integral in the last line of eq. (2.15). This choice corresponds to using the equation of motion $k^0 = |\vec{k}|$ to simplify $\mathcal{A}(k^0)$ before (rather than after) carrying out the bubble sum in Borel space. Because eq. (2.15) involves an integral over offshell momenta $k^2 \neq 0$, these choices lead to different results, with or without the $(\sin^2 \theta_k)^{-u}$ factor. Since the EEC has linear terms in k^0 , one must use the equations of motion after the bubble sum, as in eq. (2.15), because higher-order terms in the series $k^0 = |\vec{k}| + k^2/(2|\vec{k}|) + \dots$ all contribute with equal weight to the renormalon. This contrasts with offshell terms in \mathcal{A} like $k^2/(p \cdot \bar{p})$, which can safely be dropped (and could only modify the residues of poles $u \geq 3/2$).

2.2.2 Borel-space result

We now insert the LO matrix element eq. (2.3), the Borel-transformed bubble propagator eq. (2.14), and the phase-space integral relation eq. (2.15) into the bubble-modified EEC cross-section eq. (2.11), and find

$$\begin{aligned} \frac{1}{\sigma_0} \frac{d\hat{\Sigma}_{\text{bub}}}{dz} &= \frac{8}{\pi^2} \frac{C_F(\mu^2 e^c)^u}{Q^4 \beta_0} \frac{\sin(u\pi)}{u\pi} \int d^3p d^3\bar{p} d^3k \delta^4(q - \sum p_i) (\sin^2 \theta_k)^{-u} \\ &\quad \times \sum_{i,j} \frac{E_i E_j}{E \bar{E} E_g^{1+2u}} \delta(z - z_{ij}) \frac{E^2 + \bar{E}^2}{(Q - 2E)(Q - 2\bar{E})}. \end{aligned} \quad (2.16)$$

We can break this integral up into two pieces. The first term comes from the choice $ij = q\bar{q}$. The second term comes from $ij = qg$ and $\bar{q}g$, which are equal by symmetry of eq. (2.16). We illustrate how to evaluate these integrals using the qg case. First, we integrate over $d^3\bar{p}$ using $\delta^3(\vec{q} - \sum \vec{p})$. Without loss of generality, we can take the quark along the \hat{l} -axis, so $\theta_k = \theta_{qg}$, and we can write $d^3p d^3k = 4\pi E^2 E_g^2 dE dE_g d\cos\theta_k d\Delta\phi$, where $\Delta\phi$ is the difference in azimuthal angle between the quark and the gluon. We carry out the angular integrals using $\delta(z - z_{qg})$. Next, we eliminate the remaining energy-conserving delta function using $d\bar{E}$. This leaves us with a single remaining integral in $E = Qx/2$.

Combining both the $q\bar{q}$ and $qg/\bar{q}g$ terms, we have

$$\begin{aligned} \frac{1}{\sigma_0} \frac{d\hat{\Sigma}_{\text{bub}}}{dz} &= \frac{C_F(\mu^2 e^c)^u}{\beta_0 Q^{2u}} \frac{\sin(u\pi)}{u\pi} \frac{1}{[z(1-z)]^{1+u}} \int_0^1 dx \frac{x(1-x)^{-2u}}{(1-xz)^{4-2u}} \\ &\quad \times \left\{ z(1-x) \left[1 - 2x + 2x^2 - 2x^3z + x^4z^2 \right] \right. \\ &\quad \left. + 2(1-z) \left[1 - 4xz + x^2(1+2z+4z^2) - 2x^3z(1+2z) + 2x^4z^2 \right] \right\}. \end{aligned} \quad (2.17)$$

It is possible to perform these integrals analytically. Writing

$$\frac{1}{\sigma_0} \frac{d\Sigma_{\text{bub}}}{dz} = \frac{C_F(\mu^2 e^c)^u}{\beta_0 Q^{2u}} \frac{\sin(u\pi)}{u\pi} \frac{1}{[z(1-z)]^{1+u}} \left(\mathcal{I}_{q\bar{q}} + 2\mathcal{I}_{qg} \right), \quad (2.18)$$

we find

$$\begin{aligned} \mathcal{I}_{q\bar{q}} &\equiv z \int_0^1 dx \frac{x(1-x)^{-2u}}{(1-xz)^{4-2u}} (1-x) \left[1 - 2x + 2x^2 - 2x^3z + x^4z^2 \right] \\ &= \frac{4u^3(1-z)^3 - 18u^2(1-z)^2 - u(1-z)(z^2 + 7z - 32) - 6(4-3z)}{6(u-2)} {}_2F_1(1, 4-2u, 5-2u, z) \\ &\quad + \frac{-8u^4(1-z)^2 + 8u^3(1-z)(5-z) + u^2(2z^2 + 50z - 86) - u(2z^2 + 15z - 90) - 36}{6(u-1)(2u-3)}, \\ \mathcal{I}_{qg} &\equiv (1-z) \int_0^1 dx \frac{x(1-x)^{-2u}}{(1-xz)^{4-2u}} \left[1 - 4xz + x^2(1+2z+4z^2) - 2x^3z(1+2z) + 2x^4z^2 \right] \\ &= \frac{4u^2(1-z)^3 - 2u(1-z)^2(7-3z) + (1-z)(4z^2 - 14z + 13)}{2(u-2)} {}_2F_1(1, 4-2u, 5-2u, z) \\ &\quad + \frac{1}{(u-1)(2u-3)(2u-1)} \left[-8u^4(1-z)^2 + 12u^3(1-z)(3-2z) - u^2(30z^2 - 88z + 60) \right] \end{aligned}$$

$$+ u(18z^2 - 55z + 42) + 4z(3 - z) - 12 \Big], \quad (2.19)$$

where ${}_2F_1(a, b, c, x)$ is the standard hypergeometric function. These results are only valid in the region $0 < z < 1$, as we have not included the full set of contributions needed to carry out the calculation at $z = 0$ and $z = 1$.

2.3 Renormalons in the EEC

We can now identify renormalons in the EEC from eq. (2.18). Recall that renormalons are poles on the positive real u -axis; given our normalization for the Borel transform, they generally appear at half-integer or integer values of u . We find that the leading renormalon appears at $u = 1/2$, associated with a pole in \mathcal{I}_{qg} but not in \mathcal{I}_{qq} . This is consistent with the picture of leading power corrections arising from the limit in which the measured gluon becomes nonperturbative. Examining the $u \rightarrow 1/2$ limit, we find

$$\begin{aligned} \left. \frac{1}{\sigma_0} \frac{d\hat{\Sigma}}{dz} \right|_{u \rightarrow 1/2} &= \frac{\text{Res}_{1/2}}{u - 1/2} + \dots \\ &= -\frac{4C_F}{\pi\beta_0} \frac{\mu e^{c/2}}{Q} \frac{1}{[z(1-z)]^{3/2}} \frac{1}{u - 1/2} + \dots, \end{aligned} \quad (2.20)$$

where the ellipses denote terms of $\mathcal{O}((u - 1/2)^0)$. We can compute the size of the ambiguity $\Delta_{1/2}$ in the $\overline{\text{MS}}$ perturbative series $d\hat{\Sigma}/dz$ associated with this renormalon. Specifically, we evaluate the inverse Borel integral over a contour encircling the pole in complex u -space:

$$\begin{aligned} \Delta_{1/2} \left(\frac{1}{\sigma_0} \frac{d\hat{\Sigma}}{dz} \right) &= \oint_{u=1/2} du \exp \left[-u \frac{4\pi}{\beta_0 \alpha_s(\mu)} \right] \frac{\text{Res}_{1/2}}{u - 1/2} \\ &= -\frac{8iC_F e^{5/6}}{\beta_0} \frac{1}{[z(1-z)]^{3/2}} \frac{\Lambda_{\text{QCD}}}{Q}. \end{aligned} \quad (2.21)$$

This result is valid for $0 < z < 1$. Note that renormalon ambiguities are always imaginary.

This form for the ambiguity in eq. (2.21) makes clear its connection to the Λ_{QCD}/Q EEC power correction. Using $\sin^3 \chi = 8[z(1-z)]^{3/2}$, we write eq. (1.2) in terms of z :

$$\frac{1}{\sigma_0} \frac{d\Sigma}{dz} = \frac{1}{\sigma_0} \frac{d\hat{\Sigma}}{dz} + \frac{1}{2[z(1-z)]^{3/2}} \frac{\bar{\Omega}_1}{Q}. \quad (2.22)$$

Thus, the z -dependence of the leading renormalon in eq. (2.20) agrees with the leading EEC power corrections derived in refs. [49, 50]. Since the left-hand side of eq. (2.22) is a renormalon-free observable, the renormalon in the perturbative series $d\hat{\Sigma}/dz$ cancels against the renormalon in the $\overline{\text{MS}}$ definition of the hadronic parameter $\bar{\Omega}_1$. We can cross-check our result for $\text{Res}_{1/2}$ with the analogous renormalon bubble-chain calculations for thrust in the dijet limit [54, 101], which allows us to infer the ambiguity

$$\Delta_{1/2}(\bar{\Omega}_1) = \Lambda_{\text{QCD}} \frac{16iC_F e^{5/6}}{\beta_0}. \quad (2.23)$$

Thus, we confirm the cancellation of ambiguities between the two terms in eq. (2.23), $\Delta_{1/2}(d\Sigma/dz) = 0$. This cross-check also provides a test of the universality of power corrections between thrust and the EEC, though we caution that the renormalon based calculation does not account for potential $\mathcal{O}(1)$ hadron-mass corrections which can potentially spoil the universality.

The EEC observable obeys certain sum rules [34, 35, 102]. A particularly simple one, which holds nonperturbatively,³ states that

$$\int_0^1 dz \frac{d\Sigma}{dz} = \sigma. \quad (2.24)$$

Equation (2.24) follows from energy conservation, $\sum_i E_i = Q$, and reflects that $d\Sigma/dz$ integrates to the total hadronic cross-section $\sigma = \sigma(e^+e^- \rightarrow X)$, just like a regular differential distribution. This cross-section only has nonperturbative corrections at $\mathcal{O}(\Lambda_{\text{QCD}}^4/Q^4)$ for massless quarks, implying that to properly treat the $z = 0$ and $z = 1$ endpoints, we must modify the function $[z(1-z)]^{-3/2}$ such that it integrates to zero. The function remains the same for $0 < z < 1$, suggesting we need a plus distribution. Because we are dealing with two singularities, at $z = 0$ and $z = 1$, we cannot determine a functional form uniquely by imposing that the integral vanishes. The residual ambiguity can be parameterized by a constant η , where $0 < \eta < 1$. Constructing standard plus distributions over the intervals $[0, \eta]$ and $[\eta, 1]$, and then recombining terms to cancel as much of the η dependence as possible, we find that the regulated z -dependence for the power correction can be written as

$$\left[[z(1-z)]^{-3/2} \right]_+ \equiv \lim_{\epsilon \rightarrow 0} \left\{ \frac{d}{dz} \theta(z-\epsilon) \theta(1-z-\epsilon) G(z) \right\} + [\delta(1-z) - \delta(z)] G(\eta), \quad (2.25)$$

where $G(z) = -G(1-z)$, and

$$G(z) = \int_z^1 dz' [z'(1-z')]^{-3/2} = \frac{2z - 2(1-z)}{z^{1/2}(1-z)^{1/2}}. \quad (2.26)$$

It is easy to confirm that $\int_0^1 dz \left[[z(1-z)]^{-3/2} \right]_+ = 0$ for any value of η . A natural choice is to require that the plus distribution be symmetric under $z \rightarrow 1-z$, implying $\eta = 1/2$ because $G(1/2) = 0$. In this case, the $G(\eta)$ term in eq. (2.25) would vanish. With this modification the formula for the EEC in $\overline{\text{MS}}$ with its leading power correction now reads

$$\frac{1}{\sigma_0} \frac{d\Sigma}{dz} = \frac{1}{\sigma_0} \frac{d\hat{\Sigma}}{dz} + \frac{1}{2 \left[[z(1-z)]^{3/2} \right]_+} \frac{\bar{\Omega}_1}{Q}. \quad (2.27)$$

While both $\mathcal{I}_{q\bar{q}}$ and \mathcal{I}_{gq} exhibit simple poles at $u = 1$, the prefactor $\sin(u\pi)$ vanishes here. Thus, the full $d\hat{\Sigma}_{\text{bub}}/dz$ has no $u = 1$ pole,

$$\left. \frac{1}{\sigma_0} \frac{d\hat{\Sigma}}{dz} \right|_{u=1} = \frac{0}{u-1} + \dots, \quad (2.28)$$

³Note that results for higher z and $(1-z)$ moments of $d\Sigma/dz$ rely on manipulations with massless four-vectors and hence can have nonperturbative corrections in QCD.

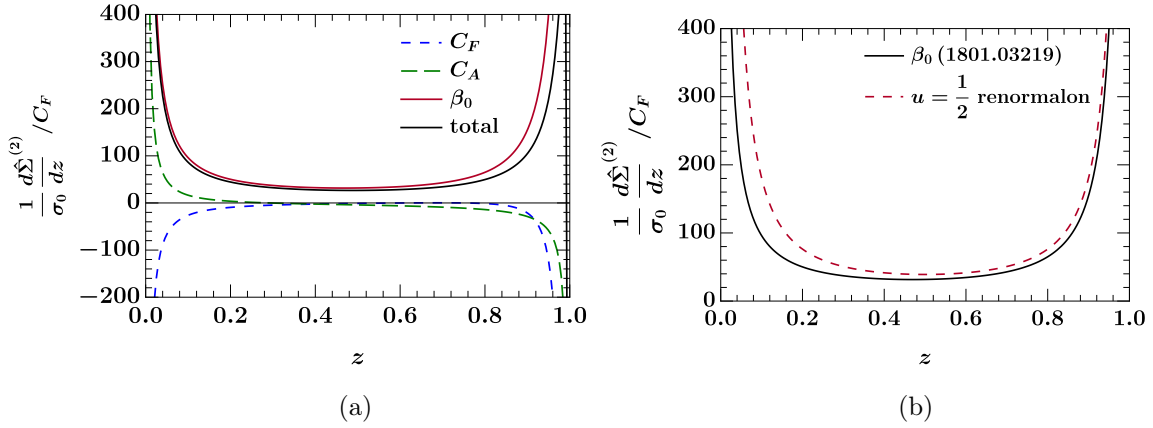


Figure 3: The $\mathcal{O}(\alpha_s^2)$ (NLO) term in the perturbative series for the EEC, as indicated by the subscript (2) on $d\hat{\Sigma}^{(2)}$. The normalization used to define this term is $\frac{d\hat{\Sigma}}{dz} = 2\left(\frac{\alpha_s}{2\pi}\right)\frac{d\hat{\Sigma}^{(1)}}{dz} + 2\left(\frac{\alpha_s}{2\pi}\right)^2\frac{d\hat{\Sigma}^{(2)}}{dz} + \dots$. We take $\mu = Qe^{-5/6}$. Figure (a) shows the results calculated in ref. [33], organized by color channels C_F^2 , $C_F C_A$, and $C_F \beta_0$, as discussed in section 2.2. The $C_F \beta_0$ term (red) dominates over the other channels. Figure (b) compares the perturbative expansion of the $u = 1/2$ renormalon in eq. (2.31) (dashed red) and the $C_F \beta_0$ term of the EEC in the $\overline{\text{MS}}$ scheme given in ref. [33] (solid black) at $\mathcal{O}(\alpha_s^2)$.

where the ellipses are $\mathcal{O}((u-1)^0)$. This means our bubble-sum analysis has no sensitivity to renormalons corresponding to $\Lambda_{\text{QCD}}^2/Q^2$ EEC power corrections. We do not, however, rule out a non-Abelian contribution to the $u = 1$ residue. The presence of $u = 1$ poles for event shape calculations which treat power corrections from the hard and collinear regions at higher orders in perturbation theory have been discussed in the literature, see for example [99, 103].

Our Borel-space result in eq. (2.18) indeed has no poles at any integer values of $u = k$, corresponding to $\Lambda_{\text{QCD}}^{2k}/Q^{2k}$ power corrections. We do observe poles at higher half-integer values, $u = k + 1/2$, associated with renormalons in $\Lambda_{\text{QCD}}^{2k+1}/Q^{2k+1}$ power corrections. Both the $\mathcal{I}_{q\bar{q}}$ and \mathcal{I}_{qg} terms contribute; for example, near $u = 3/2$, we find

$$\left. \frac{1}{\sigma_0} \frac{d\hat{\Sigma}}{dz} \right|_{u=3/2} = \frac{C_F}{\pi\beta_0} \frac{\mu^3 e^{3c/2}}{Q^3} \frac{(2-5z+4z^2)}{[z(1-z)]^{3/2}} \frac{1}{u-3/2} + \dots, \quad (2.29)$$

where the ellipses are $\mathcal{O}((u-3/2)^0)$. Note that our calculational procedure renders the residues of $u \geq 3/2$ poles somewhat ambiguous because we used $k^2 = 0$ to simplify the LO matrix element in eq. (2.3). If we had instead expanded around $k^2 = 0$, the higher-order terms $\mathcal{O}(k^{2j}/Q^{2j})$ would modify residues at $u \geq 3/2$ (but not at $u = 1/2$ or $u = 1$).

2.3.1 Renormalon series in $\overline{\text{MS}}$

Next, we investigate the manifestation of renormalons in $\overline{\text{MS}}$ perturbative calculations. Recall from figure 3a that the dominant contribution to the EEC comes from the $C_F \beta_0$ color structure at $\mathcal{O}(\alpha_s^2)$ [33]. We determine the extent to which the $u = 1/2$ pole approximates

the full $C_F\beta_0$ contribution by expanding about $u = 0$. To retain the leading logarithmic μ -independence when expanding in u , we replace $\text{Res}_{1/2} \rightarrow -\frac{1}{\beta_0} \mathcal{Z} \exp[2u \ln(\mu e^{c/2}/Q)]$ (which simplifies back to $\text{Res}_{1/2} = -\frac{1}{\beta_0} \mathcal{Z} \mu e^{c/2}/Q$ at $u=1/2$), and we also expand this exponential. Here $\mathcal{Z} = 4C_F[z(1-z)]^{-3/2}/\pi$. This gives

$$\left. \frac{1}{\sigma_0} \frac{d\hat{\Sigma}}{dz}(u) \right|_{\text{ren.}} = \frac{\text{Res}_{1/2}}{u - 1/2} \approx \frac{\mathcal{Z}}{\beta_0} \left[2 + 4u(1 + L_Q) + 8u^2(1 + L_Q + \frac{1}{2}L_Q^2) + \dots \right], \quad (2.30)$$

where $L_Q = \ln(\mu e^{c/2}/Q)$. Using the inverse Borel transform in eq. (1.4),

$$\begin{aligned} \left. \frac{1}{\sigma_0} \frac{d\hat{\Sigma}}{dz}(\alpha_s) \right|_{\text{ren.}} &= \frac{\mathcal{Z}}{\beta_0} \sum_{n=1}^{\infty} 2^n \Gamma(n) \left(\frac{\alpha_s(\mu)\beta_0}{4\pi} \right)^n \sum_{k=0}^{n-1} \frac{L_Q^k}{k!} \\ &= \frac{\mathcal{Z}}{\beta_0} \left[2 \frac{\alpha_s(\mu)\beta_0}{4\pi} + 4 \left(\frac{\alpha_s(\mu)\beta_0}{4\pi} \right)^2 (1 + L_Q) + \dots \right]. \end{aligned} \quad (2.31)$$

In figure 3b, we compare the perturbative $C_F\beta_0\alpha_s^2$ result from ref. [33] to the $\mathcal{O}(\alpha_s^2)$ renormalon term in eq. (2.31), taking $\mu = Qe^{-c/2}$ so that $L_Q = 0$. We see that the renormalon prediction mirrors the full $C_F\beta_0$ perturbative result in a substantial portion of z -space. This evidentiates the importance of taming terms in eq. (2.31) at higher orders, which grow as $2^n(n-1)!$.

3 Mitigating renormalon effects with an R scheme

In this section, we reorganize the perturbative and nonperturbative corrections to EEC, to remove leading renormalon effects from both of these terms. This leads to improved perturbative convergence and a better agreement with experimental data.

3.1 EEC in the R scheme

It is possible to systematically mitigate renormalon effects by switching from the $\overline{\text{MS}}$ scheme to a so-called R renormalization scheme [58, 93]. This scheme change removes the dominant Borel pole from the perturbative series, and also modifies matrix elements like $\bar{\Omega}_1$. The full perturbative series for the EEC in the $\overline{\text{MS}}$ scheme is

$$\frac{1}{\sigma_0} \frac{d\hat{\Sigma}}{dz} = \sum_{n=1}^{\infty} c_n(z, \mu/Q) \left[\frac{\alpha_s(\mu)}{4\pi} \right]^n, \quad (3.1)$$

where c_n is a function of z and μ/Q , eq. (2.5) gives c_1 , and ref. [33] gives c_2 analytically. To remove the $u = 1/2$ renormalon, we define an R scheme using a new subtraction scale R . In the R scheme, the leading power correction is [54, 104]

$$\Omega_1(R) = \bar{\Omega}_1 - \bar{\delta}(R). \quad (3.2)$$

Here $\bar{\delta}(R)$ is a perturbative series that removes the leading renormalon,

$$\bar{\delta}(R) = R \sum_{n=1}^{\infty} d_{n0} \left[\frac{\alpha_s(R)}{4\pi} \right]^n = R \sum_{n=1}^{\infty} d_n(\mu/R) \left[\frac{\alpha_s(\mu)}{4\pi} \right]^n, \quad (3.3)$$

where d_{n0} are numbers and $d_n(\mu/R)$ are simple functions $d_n(\mu/R) = \sum_{j=0}^{n-1} d_{nj} \ln^j(\mu/R)$. For $j \geq 1$, $d_{nj} = (2/j) \sum_{k=j}^{n-1} k d_{k(j-1)} \beta_{n-k-1}$, where the QCD β -function coefficients β_n are defined by $\mu \frac{d}{d\mu} \alpha_s(\mu) = -2\alpha_s \sum_{n=0}^{\infty} \beta_n \alpha_s^{n+1} / (4\pi)^{n+1}$. To ensure that the scheme change in eq. (3.2) does not modify the parametric size of the power correction $\bar{\Omega}_1$, we choose R such that $\bar{\delta}(R) \sim \Lambda_{\text{QCD}}$. A typical choice is $R \simeq 2 \text{ GeV}$. In the bubble-sum approximation, the coefficients at large n grow due to the $u = 1/2$ renormalon as $d_{n+1}(\mu/R) \simeq (\mu/R) n! (2\beta_0)^n Z$, for constant Z , in agreement with eq. (2.31).

There are multiple possible choices for the d_{n0} coefficients that remove the $u = 1/2$ renormalon; refs. [54, 59, 101, 104] introduce suitable schemes using the hemisphere or thrust soft functions. We follow the definition of ref. [59], whose coefficients d_{n0} stem from perturbatively expanding the logarithm of the position-space thrust soft function, $\ln \tilde{S}_{\tau_2}(y, \mu)$, and evaluating it at $iy = 1/\mu = 1/R$. Universality implies that this perturbative series has the desired renormalon, and this scheme choice does not rely on the bubble-sum approximation since it contains terms with all allowed color structures. Numerically, the first two coefficients in the scheme of ref. [59] are

$$\begin{aligned} d_1(\mu/R) &= d_{10} = -8.357, \\ d_2(\mu/R) &= d_{20} + 2\beta_0 d_{10} \ln\left(\frac{\mu}{R}\right) = -72.443 - 16.713\beta_0 \ln\left(\frac{\mu}{R}\right). \end{aligned} \quad (3.4)$$

Calculating d_{30} requires the non-logarithmic term in the $\mathcal{O}(\alpha_s^3)$ thrust soft function, for which only estimates exist [105]. Note that the $d_i(\mu/R)$ coefficients are independent of hadron masses and are therefore suitable for removing the renormalon from $\bar{\Omega}_1$ for all observables related by massless universality.

We must also change the EEC perturbative series to the R scheme:

$$\frac{1}{\sigma_0} \frac{d\hat{\Sigma}^{\text{R}}(R)}{dz} = \sum_{n=1}^{\infty} \left\{ c_n(z, \mu/Q) + \frac{R}{2Q} \frac{d_n(\mu/R)}{[z(1-z)]^{3/2}} \right\} \left[\frac{\alpha_s(\mu)}{4\pi} \right]^n. \quad (3.5)$$

Here, the $u = 1/2$ renormalon cancels order-by-order between the c_n and d_n series. This perturbative R scheme result depends both on the use of the standard $\overline{\text{MS}}$ scheme for the coupling $\alpha_s(\mu)$, and on the R scheme for the power correction. When carrying out the R scheme change on the full EEC observable, we have:

$$\frac{1}{\sigma_0} \frac{d\Sigma}{dz} = \frac{1}{\sigma_0} \frac{d\hat{\Sigma}^{\text{R}}(R)}{dz} + \frac{1}{2[[z(1-z)]^{3/2}]_+} \frac{\Omega_1(R)}{Q}. \quad (3.6)$$

This represents an improvement over the $\overline{\text{MS}}$ EEC in eq. (2.22): here, neither the perturbative series in the first term nor the power correction in the second term has a $u=1/2$ renormalon.⁴ Notably, this renormalon removal relies on the predicted z -dependence of the power correction, but *does not* rely on the bubble-sum approximation of the residue. Indeed, it captures and subtracts even non-Abelian contributions to the renormalon.

⁴One can conceptualize changing to an R scheme as locating a resurgence-pair of ambiguities in the perturbative and nonperturbative sectors of a trans-series, and shuffling the ambiguities so they cancel out.

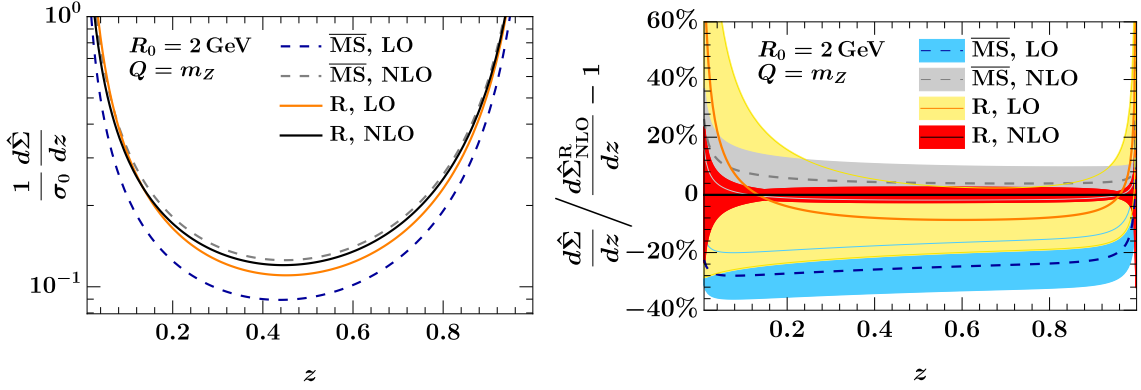


Figure 4: Comparison of perturbative results for the EEC cross-section in the $\overline{\text{MS}}$ and R schemes in eqs. (2.23) and (3.6), respectively. Here, LO is $\mathcal{O}(\alpha_s)$ and NLO is $\mathcal{O}(\alpha_s^2)$. The R scheme results have overlapping uncertainty bands and better convergence than $\overline{\text{MS}}$.

3.2 R scheme with resummation

Equation (3.6) still has one remaining issue, associated with large logarithms induced by the scale R . To avoid large logarithms in $c_n(z, \mu/Q)$ and $d_n(\mu/R)$, we see from eq. (3.5) that we would need $R \simeq \mu \simeq Q$. Retaining the scaling $\Omega_1(R) \sim \Lambda_{\text{QCD}}$, however, requires a relatively small value of R , like $R \simeq 2 \text{ GeV}$; and this scale would cause large $\ln(\mu/R) \simeq \ln(Q/R)$ in $d_n(\mu/R)$. We can resolve these conflicting needs by using the RGE for R in ref. [104], which has been implemented for $\Omega_1(R)$ in refs. [54, 59],

$$\Omega_1(R_1) = \Omega_1(R_0) + K(R_1, R_0) = \Omega_1(R_0) - \sum_{n=0}^{\infty} \gamma_n^{\Omega_1, R} \int_{R_0}^{R_1} dR \left[\frac{\alpha_s(R)}{4\pi} \right]^{n+1}. \quad (3.7)$$

Here $K(R_1, R_0)$ is a dimension-1 evolution kernel that sums large logarithms between R_0 and R_1 . For leading logarithmic (LL) resummation, we need the anomalous dimension $\gamma_0^{\Omega_1, R} = d_{10} = -8.357$, while at next-to-leading logarithmic (NLL), we also need $\gamma_1^{\Omega_1, R} = d_{20} - 2\beta_0 d_{10} = 55.693$. Here, we again quote numerical values from ref. [59], with $n_f = 5$ active light flavors, suitable for the $Q = m_Z$ that we use in our numerical analysis. Calculating $\gamma_2^{\Omega_1, R}$ requires d_{30} as input, which is not yet available.

This solution to the R -RGE enables us to write

$$\frac{1}{\sigma_0} \frac{d\Sigma}{dz} = \left[\frac{1}{\sigma_0} \frac{d\hat{\Sigma}^R(R_1)}{dz} + \frac{K(R_1, R_0)}{2Q[z(1-z)]^{3/2}} \right] + \frac{\Omega_1(R_0)}{2Q[z(1-z)]^{3/2}}_+, \quad (3.8)$$

where the first term in square brackets corresponds to the resummed perturbative prediction for the EEC, while the last term contains the R scheme power correction. Here, $R_0 \simeq 2 \text{ GeV}$ and $R_1 \simeq Q$.

3.3 Perturbative convergence

Next, we compute the R scheme perturbative EEC cross-section $d\hat{\Sigma}^R/dz$ at LO and NLO from eq. (3.5). For simplicity, we take $\mu = R_1$ in $d\hat{\Sigma}^R/dz$. At LO, we carry out the

resummation in $K(R_1, R_0)$ at NLL using $\gamma_{0,1}^{\Omega_1, R}$. At NLO, one should use K at NNLL order; however, $\gamma_2^{\Omega_1, R}$ is not yet known, so we use K at NLL. Based on previous R-RGE studies [58, 93, 106], we anticipate that the NNLL kernel would lead to only slightly smaller perturbative uncertainties at NLO.

In figure 4, we set $Q = m_Z$ and $\alpha_s(m_Z) = 0.118$, and use $R_0 = 2 \text{ GeV}$ for the R scheme.⁵ We assess the uncertainty from higher-order perturbative corrections in the conventional manner, by varying the renormalization scale dependences μ in $\overline{\text{MS}}$ and $R_1 = \mu$ in R scheme, both on the range $Q/2$ to $2Q$, using the LL and NLL running of $\alpha_s(\mu)$ at LO and NLO, respectively. In the left panel of figure 4, we show central values; in the right panel, we show deviation from the NLO R scheme curve and also include perturbative uncertainties. The $\overline{\text{MS}}$ EEC value increases significantly from LO to NLO, and the NLO curve is not within the estimated LO uncertainty. In contrast, the R scheme exhibits improved convergence, with NLO results contained within the LO uncertainty band. Furthermore, the estimated perturbative uncertainty at NLO is about a factor of two smaller for the R scheme than for $\overline{\text{MS}}$. Note that (numerical) results exist for the EEC at NNLO= $\mathcal{O}(\alpha_s^3)$ in the $\overline{\text{MS}}$ scheme [31, 32], and these results lie just above the upper edge of the NLO $\overline{\text{MS}}$ uncertainty band for almost all values of z . We do not analyze these results here as corresponding NNLO R scheme results are not yet available.

Note that so far, we have only considered the EEC perturbative series, i.e. the first $\overline{\text{MS}}$ term in eq. (2.27) and the bracketed R scheme terms in eq. (3.8). We do not expect these series to asymptote to the same value, as the nonperturbative parameters $\bar{\Omega}_1$ and $\Omega_1(R_0)$ differ.

3.4 Nonperturbative corrections and hadron masses

To make a more complete prediction for the EEC that includes nonperturbative information, we capitalize on the universality between the thrust and EEC power corrections. Ref. [54] determined the thrust power corrections $\bar{\Omega}_1$ and $\Omega_1(R_0)$ by fits to data. These fits also yielded $\alpha_s(m_Z) = 0.114$, which for consistency we use throughout this section, along with $R_0 = 2 \text{ GeV}$. At $\text{N}^3\text{LL}' + \mathcal{O}(\alpha_s^3)$ order, they obtained $\bar{\Omega}_1 = 0.252 \pm 0.069 \text{ GeV}$ and $\Omega_1^{\text{ref.}[51]}(R_0) = 0.323 \pm 0.045$, which translates to $\Omega_1(R_0) = 0.739 \pm 0.045 \text{ GeV}$ in the R scheme of ref. [59] used here.⁶

If we treat all hadrons as massless, then universality implies that $\bar{\Omega}_1$ and $\Omega_1(R)$ are the same for both thrust and the EEC [49, 50, 55]. Since Ω_1 is the vacuum matrix element of a measurement operator sandwiched by back-to-back lightcone Wilson lines, power corrections for such observables are related by boost symmetry [55]. The assumption that hadrons are massless enters such calculations when manipulating kinematic variables to translate between energies, momenta, rapidity, and angles.

⁵A useful feature of R schemes is that the cutoff R_0 dependence cancels between the perturbative result and the Ω_1 power correction in eq. (3.8). If we leave out Ω_1 , we can estimate the size of this power correction by varying R_0 in the perturbative term. We do not make use of this method here.

⁶Compared to eq. (3.4), the scheme of ref. [54] has $d_{10} = 0$ and non-zero results only at higher orders, which is the main cause of this numerical difference.

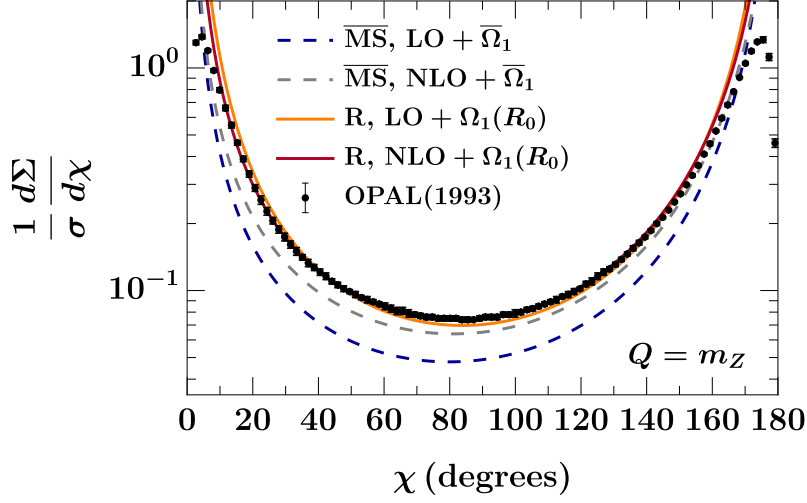


Figure 5: Predictions for the full EEC with the inclusion of the leading nonperturbative correction in the $\overline{\text{MS}}$ and R schemes, compared to OPAL data [60], as discussed in section 3.4. Central values are displayed at both $\text{LO}=\mathcal{O}(\alpha_s)$ and $\text{NLO}=\mathcal{O}(\alpha_s^2)$.

Hadron mass corrections are known to have a significant impact on universality relations for Ω_1 [56]. This is influenced by assumptions made about hadron masses when using experimental measurements to determine a given observable. Ref. [57] developed a field-theoretic method to compute hadron mass corrections to universality relations. For an observable e , we denote the leading-power mass correction by $\Omega_1^e = c_e \Omega_1^{g_e}$, where $\Omega_1^{g_e} = \int_0^1 dr g_e(r) \Omega_1(r)$ and $r = p_T / \sqrt{p_T^2 + m^2}$ for a hadron of transverse momentum p_T and mass m . Here c_e and $g_e(r)$ are analytically calculable terms, while $\Omega_1(r)$ is a universal hadronic matrix element. Following the notation of ref. [57], for the EEC we define

$$f_{\text{EEC}}(r, y) = 2 \cosh y \delta \left(\frac{1 - \cos \theta}{2} - z \right) = 2 \cosh y \delta \left(\frac{1}{2} - \frac{\sinh y}{2\sqrt{r^2 + \sinh^2 y}} - z \right). \quad (3.9)$$

Here, y is rapidity and the prefactor 2 is the combinatoric factor for two energies. Then,

$$\begin{aligned} c_{\text{EEC}} &= \int_{-\infty}^{+\infty} dy f_{\text{EEC}}(1, y) = \frac{1}{2[z(1-z)]^{3/2}}, \\ g_{\text{EEC}}(r) &= \frac{1}{c_{\text{EEC}}} \int_{-\infty}^{+\infty} dy f_{\text{EEC}}(r, y) = r. \end{aligned} \quad (3.10)$$

Here, c_{EEC} is the coefficient of Ω_1 for the massless universality relation, in agreement with eqs. (2.27) and (3.8).

The result $g_{\text{EEC}}(r) = r$ implies that $\Omega_1^{g_{\text{EEC}}}$ is in the so-called E-scheme universality class of power corrections, which differs from the thrust universality class $\Omega_1^{g_\tau}$ quoted above. Since $g_{\text{EEC}}(r) > g_\tau(r)$, we expect the value of the EEC power correction to be larger than that for thrust. A two-term basis expansion provides a fairly accurate parametrization for the impact of hadron masses on $g(r)$ [57], enabling us to write any observable as a linear

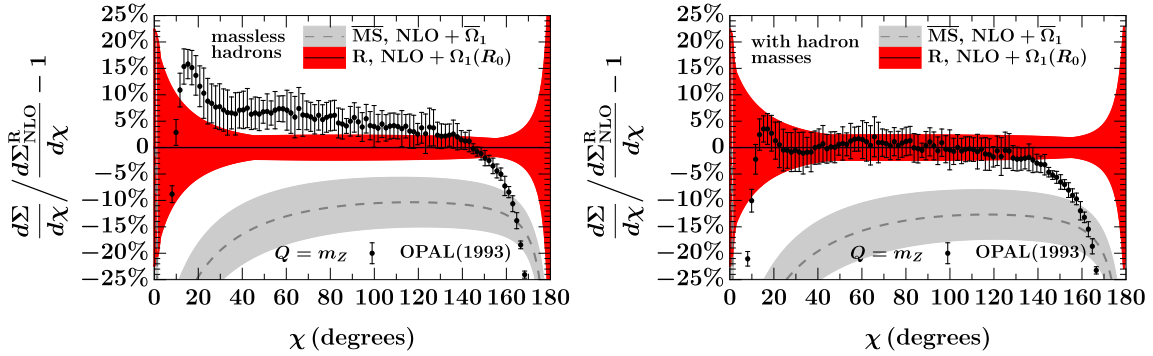


Figure 6: Full nonperturbative predictions for the EEC without (left) and with (right) corrections from hadron mass effects as discussed in sections 3.4 and 3.5, normalized to NLO R scheme. We show the uncertainty bands for NLO curves with the perturbative and parametric uncertainties added in quadrature.

combination of nonperturbative parameters $\Omega_1^{g_e} = b_0^e \Omega_1^{(0)} + b_1^e \Omega_1^{(1)}$. Using the R scheme thrust fit, and $\Omega_1^{(0)} - \Omega_1^{(1)} \simeq 0.7 \text{ GeV}$ from Monte Carlo fits [57], we find $\Omega_1^{g_{\text{EEC}}}/\Omega_1^{g_\tau} = 1.21$. Thus, hadron mass effects in the EEC induce a 21% increase in the value of $\Omega_1(R_0)$, giving $\Omega_1^{g_{\text{EEC}}}(R_0) = 0.895 \pm 0.054 \text{ GeV}$. It is harder to obtain an analogous $\overline{\text{MS}}$ estimate, as Monte Carlo simulations with hadronization at the shower cutoff are physically similar to the R scheme, but not to $\overline{\text{MS}}$. Thus, we simply assume that $\overline{\text{MS}}$ hadron mass corrections also cause a 21% increase, yielding $\bar{\Omega}_1^{g_{\text{EEC}}} = 0.305 \pm 0.084 \text{ GeV}$.

3.5 Comparison to experimental data

We now combine the perturbative EEC results and leading nonperturbative corrections to predict the total EEC cross-section. In figure 5, we compare our $\overline{\text{MS}}$ and R scheme results with OPAL data [60]. Here, $\bar{\Omega}_1$ and $\Omega_1(R_0)$ include the estimated hadron mass corrections. We normalize the theory results by dividing by the full hadronic cross-section σ , to $\mathcal{O}(\alpha_s)$ and $\mathcal{O}(\alpha_s^2)$ for LO and NLO [107]. Our NLO R scheme result agrees well with OPAL data, except in the $z \rightarrow 0$ and $z \rightarrow 1$ regions, where one should resum large perturbative logarithms to higher orders in α_s . Note that the NLO R scheme result is also closer to the data than the LO R scheme result. For $\overline{\text{MS}}$, the power correction shifts $\overline{\text{MS}}$ predictions closer to the data, but it is apparent that one needs higher-order perturbative corrections to improve agreement.

It is difficult to illustrate hadron mass effects and uncertainties in the theoretical predictions on the scales shown in figure 5. Therefore, we display the same data as percent deviations from the NLO R scheme result in figure 6. In the left panel, we use the massless hadron parameter values, corresponding to the thrust fit values of $\bar{\Omega}_1$ and $\Omega_1(R_0)$.⁷ In the right panel, we include the 21% increase in these parameters due to the hadron mass effects

⁷Though we have only shown predictions for the EEC and not considered fits to the EEC data, we do note that fits at a single value of Q are insufficient to break the degeneracy between different values of $\alpha_s(m_Z)$ and $\Omega_1(R_0)$. For example, had we fixed $\alpha_s(m_Z) = 0.118$, we could find a value of $\Omega_1(R_0)$ that gives similarly good agreement with the OPAL data, as in the right panel of figure 6.

discussed in [section 3.4](#); we find that this strongly improves the agreement between theory and data in both normalization and shape. We show both the perturbative uncertainties at NLO from varying μ and R_1 and the parametric uncertainties from the fit used to obtain values for $\Omega_1(R_0)$ and $\bar{\Omega}_1$, quoted in [section 3.4](#). These two types of uncertainties are added in quadrature in [figure 6](#). We note that the $\overline{\text{MS}}$ perturbative uncertainty is about twice as large as the parametric uncertainty of $\bar{\Omega}_1$, and the R scheme perturbative uncertainty is of similar size as the parametric uncertainty of $\Omega_1(R_0)$. We also remark that in all cases the power corrections give improved agreement with data compared to the purely perturbative EEC. Furthermore, in the R scheme, the fixed-order result using a single $R = R_0 = R_1$ and resummation kernel $K = 0$ exhibits worse convergence and worse agreement with data than the NLO R scheme result shown here.

4 Concluding remarks

Energy correlators show great promise for extracting a breadth of information about QCD from colliders. To fully capitalize on the opportunity presented by this class of observables, one must reach a high level of precision in both perturbative calculations and nonperturbative corrections. In this paper, we analyzed renormalons in the $\overline{\text{MS}}$ EEC to investigate the nature of its asymptotic perturbative series, and we converted our results to an R scheme that removes the leading renormalon ambiguity, significantly improving convergence and agreement with experimental data. Specifically, we computed the Borel space $\overline{\text{MS}}$ EEC in the bubble-sum approximation, allowing us to calculate the z -dependence of the leading $u = 1/2$ renormalon pole. We confirmed the expected $[z(1 - z)]^{-3/2}$ dependence of the corresponding $\mathcal{O}(\Lambda_{\text{QCD}}/Q)$ power correction, and showed how to regulate the $z \rightarrow 0$ and $z \rightarrow 1$ endpoints. We found no $u = 1$ pole under this approximation. Next, we constructed an R renormalization scheme that removes the leading $u = 1/2$ renormalon from both the perturbative and the nonperturbative contributions to the EEC, with explicit results given to $\mathcal{O}(\alpha_s^2)$. This scheme change significantly improves the convergence of the EEC perturbative series and brings theoretical calculations of the EEC into reasonable agreement with experimental data already at $\mathcal{O}(\alpha_s^2)$. This paper lays the groundwork for improving theoretical predictions for other EEC observables, such as higher-point EEC correlators (see e.g. [ref. \[4\]](#)) and EEC observables relevant for electron-ion and hadron-hadron colliders. It would also be interesting to extend the analysis here to make use of the $\mathcal{O}(\alpha_s^3)$ $\overline{\text{MS}}$ perturbative results for the two-point EEC [\[31, 32\]](#).

Acknowledgments

We thank Andre Hoang, Kyle Lee, Johannes Michel, Ian Moult, Michael Ogilvie, and Aditya Pathak for helpful conversations. This work was supported by the U.S. Department of Energy, Office of Science, Office of Nuclear Physics from DE-SC0011090. I.S. was also supported in part by the Simons Foundation through the Investigator grant 327942. S.T.S. was partially supported by the U.S. National Science Foundation through a Graduate Research Fellowship under Grant No. 1745302, and fellowships from the MIT Department of

Physics and MIT School of Science. Z.S. was also supported by a fellowship from the MIT Department of Physics.

References

- [1] C. L. Basham, L. S. Brown, S. D. Ellis and S. T. Love, *Energy correlations in electron-positron annihilation: Testing quantum chromodynamics*, *Phys. Rev. Lett.* **41** (1978) 1585.
- [2] C. L. Basham, L. S. Brown, S. D. Ellis and S. T. Love, *Energy correlations in electron-positron annihilation in quantum chromodynamics: Asymptotically free perturbation theory*, *Phys. Rev. D* **19** (1979) 2018.
- [3] A. Ali, E. Pietarinen and W. J. Stirling, *Transverse Energy-energy Correlations: A Test of Perturbative QCD for the Proton - Anti-proton Collider*, *Phys. Lett. B* **141** (1984) 447.
- [4] H. Chen, M.-X. Luo, I. Moulton, T.-Z. Yang, X. Zhang and H. X. Zhu, *Three point energy correlators in the collinear limit: symmetries, dualities and analytic results*, *JHEP* **08** (2020) 028 [[1912.11050](#)].
- [5] H. T. Li, Y. Makris and I. Vitev, *Energy-energy correlators in Deep Inelastic Scattering*, *Phys. Rev. D* **103** (2021) 094005 [[2102.05669](#)].
- [6] H. T. Li, I. Vitev and Y. J. Zhu, *Transverse-Energy-Energy Correlations in Deep Inelastic Scattering*, *JHEP* **11** (2020) 051 [[2006.02437](#)].
- [7] H. Chen, I. Moulton, X. Zhang and H. X. Zhu, *Rethinking jets with energy correlators: Tracks, resummation, and analytic continuation*, *Phys. Rev. D* **102** (2020) 054012 [[2004.11381](#)].
- [8] P. T. Komiske, I. Moulton, J. Thaler and H. X. Zhu, *Analyzing N-Point Energy Correlators inside Jets with CMS Open Data*, *Phys. Rev. Lett.* **130** (2023) 051901 [[2201.07800](#)].
- [9] K. Lee, B. Meçaj and I. Moulton, *Conformal Colliders Meet the LHC*, [2205.03414](#).
- [10] D. Neill, G. Vita, I. Vitev and H. X. Zhu, *Energy-Energy Correlators for Precision QCD*, in *2022 Snowmass Summer Study*, 3, 2022, [2203.07113](#).
- [11] P. N. Burrows, H. Masuda, D. Muller and Y. Ohnishi, *Application of 'optimized' perturbation theory to determination of $\alpha_s M(Z)^{**2}$ from hadronic event shape observables in $e^+ e^-$ annihilation*, *Phys. Lett. B* **382** (1996) 157 [[hep-ph/9602210](#)].
- [12] A. Kardos, S. Kluth, G. Somogyi, Z. Tulipánt and A. Verbytskyi, *Precise determination of $\alpha_s(M_Z)$ from a global fit of energy-energy correlation to NNLO+NNLL predictions*, *Eur. Phys. J. C* **78** (2018) 498 [[1804.09146](#)].
- [13] A. Gao, H. T. Li, I. Moulton and H. X. Zhu, *Precision QCD Event Shapes at Hadron Colliders: The Transverse Energy-Energy Correlator in the Back-to-Back Limit*, *Phys. Rev. Lett.* **123** (2019) 062001 [[1901.04497](#)].
- [14] OPAL collaboration, M. Z. Akrawy et al., *A Measurement of energy correlations and a determination of $\alpha_s(M_Z)$ in $e^+ e^-$ annihilations at $s^{**}(1/2) = 91\text{-GeV}$* , *Phys. Lett. B* **252** (1990) 159.
- [15] ALEPH collaboration, D. Decamp et al., *Measurement of α_s from the structure of particle clusters produced in hadronic Z decays*, *Phys. Lett. B* **257** (1991) 479.
- [16] L3 collaboration, B. Adeva et al., *Determination of α_s from energy-energy correlations measured on the Z^0 resonance.*, *Phys. Lett. B* **257** (1991) 469.

- [17] ATLAS collaboration, G. Aad et al., *Measurement of transverse energy-energy correlations in multi-jet events in pp collisions at $\sqrt{s} = 7$ TeV using the ATLAS detector and determination of the strong coupling constant $\alpha_s(m_Z)$* , *Phys. Lett. B* **750** (2015) 427 [[1508.01579](#)].
- [18] ATLAS collaboration, M. Aaboud et al., *Determination of the strong coupling constant α_s from transverse energy-energy correlations in multijet events at $\sqrt{s} = 8$ TeV using the ATLAS detector*, *Eur. Phys. J. C* **77** (2017) 872 [[1707.02562](#)].
- [19] ATLAS collaboration, *Determination of the strong coupling constant and test of asymptotic freedom from Transverse Energy-Energy Correlations in multijet events at $\sqrt{s} = 13$ TeV with the ATLAS detector*, .
- [20] SLD collaboration, K. Abe et al., *Measurement of alpha-s from energy-energy correlations at the Z0 resonance*, *Phys. Rev. D* **50** (1994) 5580 [[hep-ex/9405006](#)].
- [21] R. Abdul Khalek et al., *Science Requirements and Detector Concepts for the Electron-Ion Collider: EIC Yellow Report*, [2103.05419](#).
- [22] H. N. Schneider, G. Kramer and G. Schierholz, *Higher Order QCD Corrections to the Energy-energy Correlation Function*, *Z. Phys. C* **22** (1984) 201.
- [23] N. K. Falck and G. Kramer, *Theoretical Studies of Energy-energy Correlation in e^+e^- Annihilation*, *Z. Phys. C* **42** (1989) 459.
- [24] E. W. N. Glover and M. R. Sutton, *The Energy-energy correlation function revisited*, *Phys. Lett. B* **342** (1995) 375 [[hep-ph/9410234](#)].
- [25] G. Kramer and H. Spiesberger, *A New calculation of the NLO energy-energy correlation function*, *Z. Phys. C* **73** (1997) 495 [[hep-ph/9603385](#)].
- [26] A. Ali and F. Barreiro, *An $O(\alpha^{-2}s^2)$ Calculation of Energy-energy Correlation in e^+e^- Annihilation and Comparison With Experimental Data*, *Phys. Lett. B* **118** (1982) 155.
- [27] A. Ali and F. Barreiro, *Energy-energy Correlations in e^+e^- Annihilation*, *Nucl. Phys. B* **236** (1984) 269.
- [28] D. G. Richards, W. J. Stirling and S. D. Ellis, *Second Order Corrections to the Energy-energy Correlation Function in Quantum Chromodynamics*, *Phys. Lett. B* **119** (1982) 193.
- [29] D. G. Richards, W. J. Stirling and S. D. Ellis, *Energy-energy Correlations to Second Order in Quantum Chromodynamics*, *Nucl. Phys. B* **229** (1983) 317.
- [30] S. Catani and M. H. Seymour, *The Dipole formalism for the calculation of QCD jet cross-sections at next-to-leading order*, *Phys. Lett. B* **378** (1996) 287 [[hep-ph/9602277](#)].
- [31] V. Del Duca, C. Duhr, A. Kardos, G. Somogyi and Z. Trócsányi, *Three-Jet Production in Electron-Positron Collisions at Next-to-Next-to-Leading Order Accuracy*, *Phys. Rev. Lett.* **117** (2016) 152004 [[1603.08927](#)].
- [32] Z. Tulipánt, A. Kardos and G. Somogyi, *Energy-energy correlation in electron-positron annihilation at NNLL + NNLO accuracy*, *Eur. Phys. J. C* **77** (2017) 749 [[1708.04093](#)].
- [33] L. J. Dixon, M.-X. Luo, V. Shtabovenko, T.-Z. Yang and H. X. Zhu, *Analytical Computation of Energy-Energy Correlation at Next-to-Leading Order in QCD*, *Phys. Rev. Lett.* **120** (2018) 102001 [[1801.03219](#)].

- [34] L. J. Dixon, I. Moult and H. X. Zhu, *Collinear limit of the energy-energy correlator*, *Phys. Rev. D* **100** (2019) 014009 [[1905.01310](#)].
- [35] G. P. Korchemsky, *Energy correlations in the end-point region*, *JHEP* **01** (2020) 008 [[1905.01444](#)].
- [36] H. Chen, T.-Z. Yang, H. X. Zhu and Y. J. Zhu, *Analytic Continuation and Reciprocity Relation for Collinear Splitting in QCD*, *Chin. Phys. C* **45** (2021) 043101 [[2006.10534](#)].
- [37] J. Kodaira and L. Trentadue, *Summing Soft Emission in QCD*, *Phys. Lett. B* **112** (1982) 66.
- [38] J. Kodaira and L. Trentadue, *Single Logarithm Effects in electron-Positron Annihilation*, *Phys. Lett. B* **123** (1983) 335.
- [39] D. de Florian and M. Grazzini, *The Back-to-back region in $e^+ e^-$ energy-energy correlation*, *Nucl. Phys. B* **704** (2005) 387 [[hep-ph/0407241](#)].
- [40] I. Moult and H. X. Zhu, *Simplicity from Recoil: The Three-Loop Soft Function and Factorization for the Energy-Energy Correlation*, *JHEP* **08** (2018) 160 [[1801.02627](#)].
- [41] M. A. Ebert, B. Mistlberger and G. Vita, *The Energy-Energy Correlation in the back-to-back limit at N^3LO and N^3LL'* , *JHEP* **08** (2021) 022 [[2012.07859](#)].
- [42] C. Duhr, B. Mistlberger and G. Vita, *Four-Loop Rapidity Anomalous Dimension and Event Shapes to Fourth Logarithmic Order*, *Phys. Rev. Lett.* **129** (2022) 162001 [[2205.02242](#)].
- [43] A. V. Belitsky, S. Hohenegger, G. P. Korchemsky, E. Sokatchev and A. Zhiboedov, *From correlation functions to event shapes*, *Nucl. Phys. B* **884** (2014) 305 [[1309.0769](#)].
- [44] A. V. Belitsky, S. Hohenegger, G. P. Korchemsky, E. Sokatchev and A. Zhiboedov, *Event shapes in $\mathcal{N} = 4$ super-Yang-Mills theory*, *Nucl. Phys. B* **884** (2014) 206 [[1309.1424](#)].
- [45] A. V. Belitsky, S. Hohenegger, G. P. Korchemsky, E. Sokatchev and A. Zhiboedov, *Energy-Energy Correlations in $N=4$ Supersymmetric Yang-Mills Theory*, *Phys. Rev. Lett.* **112** (2014) 071601 [[1311.6800](#)].
- [46] J. M. Henn, E. Sokatchev, K. Yan and A. Zhiboedov, *Energy-energy correlation in $N=4$ super Yang-Mills theory at next-to-next-to-leading order*, *Phys. Rev. D* **100** (2019) 036010 [[1903.05314](#)].
- [47] I. Moult, G. Vita and K. Yan, *Subleading power resummation of rapidity logarithms: the energy-energy correlator in $\mathcal{N} = 4$ SYM*, *JHEP* **07** (2020) 005 [[1912.02188](#)].
- [48] P. Nason and M. H. Seymour, *Infrared renormalons and power suppressed effects in $e^+ e^-$ jet events*, *Nucl. Phys. B* **454** (1995) 291 [[hep-ph/9506317](#)].
- [49] G. P. Korchemsky and G. F. Sterman, *Power corrections to event shapes and factorization*, *Nucl. Phys. B* **555** (1999) 335 [[hep-ph/9902341](#)].
- [50] A. V. Belitsky, G. P. Korchemsky and G. F. Sterman, *Energy flow in QCD and event shape functions*, *Phys. Lett. B* **515** (2001) 297 [[hep-ph/0106308](#)].
- [51] Y. L. Dokshitzer, G. Marchesini and B. R. Webber, *Nonperturbative effects in the energy energy correlation*, *JHEP* **07** (1999) 012 [[hep-ph/9905339](#)].
- [52] Y. L. Dokshitzer, A. Lucenti, G. Marchesini and G. P. Salam, *On the universality of the Milan factor for $1/Q$ power corrections to jet shapes*, *JHEP* **05** (1998) 003 [[hep-ph/9802381](#)].

- [53] Y. L. Dokshitzer, A. Lucenti, G. Marchesini and G. P. Salam, *Universality of $1/Q$ corrections to jet-shape observables rescued*, *Nucl. Phys. B* **511** (1998) 396 [[hep-ph/9707532](#)].
- [54] R. Abbate, M. Fickinger, A. H. Hoang, V. Mateu and I. W. Stewart, *Thrust at N^3LL with Power Corrections and a Precision Global Fit for $\alpha_s(m_Z)$* , *Phys.Rev.* **D83** (2011) 074021 [[1006.3080](#)].
- [55] C. Lee and G. Sterman, *Momentum flow correlations from event shapes: Factorized soft gluons and soft-collinear effective theory*, *Phys. Rev.* **D75** (2007) 014022 [[hep-ph/0611061](#)].
- [56] G. P. Salam and D. Wicke, *Hadron masses and power corrections to event shapes*, *JHEP* **05** (2001) 061 [[hep-ph/0102343](#)].
- [57] V. Mateu, I. W. Stewart and J. Thaler, *Power Corrections to Event Shapes with Mass-Dependent Operators*, *Phys. Rev. D* **87** (2013) 014025 [[1209.3781](#)].
- [58] A. H. Hoang, A. Jain, I. Scimemi and I. W. Stewart, *R-evolution: Improving perturbative QCD*, *Phys. Rev. D* **82** (2010) 011501 [[0908.3189](#)].
- [59] B. Bachu, A. H. Hoang, V. Mateu, A. Pathak and I. W. Stewart, *Boosted top quarks in the peak region with $NL3L$ resummation*, *Phys. Rev. D* **104** (2021) 014026 [[2012.12304](#)].
- [60] OPAL collaboration, P. D. Acton et al., *A Determination of $\alpha_s(M(Z^0))$ at LEP using resummed QCD calculations*, *Z. Phys. C* **59** (1993) 1.
- [61] F. J. Dyson, *Divergence of perturbation theory in quantum electrodynamics*, *Phys. Rev.* **85** (1952) 631.
- [62] C. M. Bender and T. T. Wu, *Anharmonic oscillator*, *Phys. Rev.* **184** (1969) 1231.
- [63] C. M. Bender and T. T. Wu, *Anharmonic oscillator. 2: A Study of perturbation theory in large order*, *Phys. Rev. D* **7** (1973) 1620.
- [64] M. Beneke, *Renormalons*, *Phys. Rept.* **317** (1999) 1 [[hep-ph/9807443](#)].
- [65] P. C. Argyres and M. Unsal, *The semi-classical expansion and resurgence in gauge theories: new perturbative, instanton, bion, and renormalon effects*, *JHEP* **08** (2012) 063 [[1206.1890](#)].
- [66] G. V. Dunne and M. Ünsal, *Generating nonperturbative physics from perturbation theory*, *Phys. Rev. D* **89** (2014) 041701 [[1306.4405](#)].
- [67] C. A. Hurst, *The Enumeration of Graphs in the Feynman-Dyson Technique*, *Proc. Roy. Soc. Lond. A* **214** (1952) 44.
- [68] C. M. Bender and T. T. Wu, *Statistical Analysis of Feynman Diagrams*, *Phys. Rev. Lett.* **37** (1976) 117.
- [69] L. N. Lipatov, *Divergence of the Perturbation Theory Series and the Quasiclassical Theory*, *Sov. Phys. JETP* **45** (1977) 216.
- [70] J. Zinn-Justin, *Perturbation Series at Large Orders in Quantum Mechanics and Field Theories: Application to the Problem of Resummation*, *Phys. Rept.* **70** (1981) 109.
- [71] C. M. Bender and S. A. Orszag, *Advanced Mathematical Methods for Scientists and Engineers I*. Springer New York, 1999, [10.1007/978-1-4757-3069-2](#).
- [72] D. J. Gross and A. Neveu, *Dynamical Symmetry Breaking in Asymptotically Free Field Theories*, *Phys. Rev. D* **10** (1974) 3235.

- [73] B. E. Lautrup, *On High Order Estimates in QED*, *Phys. Lett. B* **69** (1977) 109.
- [74] G. 't Hooft, *Can We Make Sense Out of Quantum Chromodynamics?*, *Subnucl. Ser.* **15** (1979) 943.
- [75] E. B. Bogomolny and V. A. Fateev, *Large Orders Calculations in the Gauge Theories*, *Phys. Lett. B* **71** (1977) 93.
- [76] A. Behtash, G. V. Dunne, T. Schaefer, T. Sulejmanpasic and M. Ünsal, *Critical Points at Infinity, Non-Gaussian Saddles, and Bions*, *JHEP* **06** (2018) 068 [[1803.11533](#)].
- [77] G. V. Dunne and M. Ünsal, *Continuity and Resurgence: towards a continuum definition of the $\mathbb{CP}(N-1)$ model*, *Phys. Rev. D* **87** (2013) 025015 [[1210.3646](#)].
- [78] A. Cherman, D. Dorigoni, G. V. Dunne and M. Ünsal, *Resurgence in Quantum Field Theory: Nonperturbative Effects in the Principal Chiral Model*, *Phys. Rev. Lett.* **112** (2014) 021601 [[1308.0127](#)].
- [79] G. Basar, G. V. Dunne and M. Ünsal, *Resurgence theory, ghost-instantons, and analytic continuation of path integrals*, *JHEP* **10** (2013) 041 [[1308.1108](#)].
- [80] G. V. Dunne and M. Ünsal, *Uniform WKB, Multi-instantons, and Resurgent Trans-Series*, *Phys. Rev. D* **89** (2014) 105009 [[1401.5202](#)].
- [81] A. Cherman, D. Dorigoni and M. Ünsal, *Decoding perturbation theory using resurgence: Stokes phenomena, new saddle points and Lefschetz thimbles*, *JHEP* **10** (2015) 056 [[1403.1277](#)].
- [82] T. Fujimori, S. Kamata, T. Misumi, M. Nitta and N. Sakai, *Bion non-perturbative contributions versus infrared renormalons in two-dimensional \mathbb{CP}^{N-1} models*, *JHEP* **02** (2019) 190 [[1810.03768](#)].
- [83] M. Ünsal, *TQFT at work for IR-renormalons, resurgence and Lefschetz decomposition*, [2106.14971](#).
- [84] J. Écalle, *Les fonctions résurgentes I-III*. Université de Paris-Sud Département de Mathématique, Orsay, 1981.
- [85] J. P. Boyd, *The Devil's Invention: Asymptotic, Supersymptotic and Hyperasymptotic Series*, *Acta Applicandae Mathematica* **56** (1999) 1.
- [86] D. Dorigoni, *An Introduction to Resurgence, Trans-Series and Alien Calculus*, *Annals Phys.* **409** (2019) 167914 [[1411.3585](#)].
- [87] I. Aniceto, G. Basar and R. Schiappa, *A Primer on Resurgent Transseries and Their Asymptotics*, *Phys. Rept.* **809** (2019) 1 [[1802.10441](#)].
- [88] A. V. Manohar and M. B. Wise, *Heavy quark physics*, vol. 10. 2000.
- [89] I. I. Y. Bigi, M. A. Shifman, N. G. Uraltsev and A. I. Vainshtein, *The Pole mass of the heavy quark. Perturbation theory and beyond*, *Phys. Rev. D* **50** (1994) 2234 [[hep-ph/9402360](#)].
- [90] M. Beneke and V. M. Braun, *Heavy quark effective theory beyond perturbation theory: Renormalons, the pole mass and the residual mass term*, *Nucl. Phys. B* **426** (1994) 301 [[hep-ph/9402364](#)].
- [91] I. I. Y. Bigi, M. A. Shifman and N. Uraltsev, *Aspects of heavy quark theory*, *Ann. Rev. Nucl. Part. Sci.* **47** (1997) 591 [[hep-ph/9703290](#)].

- [92] A. Pineda, *Determination of the bottom quark mass from the Upsilon(1S) system*, *JHEP* **06** (2001) 022 [[hep-ph/0105008](#)].
- [93] A. H. Hoang, A. Jain, I. Scimemi and I. W. Stewart, *Infrared Renormalization Group Flow for Heavy Quark Masses*, *Phys. Rev. Lett.* **101** (2008) 151602 [[0803.4214](#)].
- [94] A. G. Grozin and M. Neubert, *Higher order estimates of the chromomagnetic moment of a heavy quark*, *Nucl. Phys. B* **508** (1997) 311 [[hep-ph/9707318](#)].
- [95] A. H. Mueller, *On the Structure of Infrared Renormalons in Physical Processes at High-Energies*, *Nucl. Phys. B* **250** (1985) 327.
- [96] M. Dasgupta and G. P. Salam, *Event shapes in e^+e^- annihilation and deep inelastic scattering*, *J. Phys. G* **30** (2004) R143 [[hep-ph/0312283](#)].
- [97] S. Fleming, A. H. Hoang, S. Mantry and I. W. Stewart, *Top Jets in the Peak Region: Factorization Analysis with NLL Resummation*, *Phys. Rev. D* **77** (2008) 114003 [[0711.2079](#)].
- [98] A. H. Hoang, D. W. Kolodrubetz, V. Mateu and I. W. Stewart, *C-parameter distribution at N^3LL' including power corrections*, *Phys. Rev. D* **91** (2015) 094017 [[1411.6633](#)].
- [99] N. G. Gracia and V. Mateu, *Toward massless and massive event shapes in the large- β_0 limit*, *JHEP* **07** (2021) 229 [[2104.13942](#)].
- [100] S. J. Brodsky, G. P. Lepage and P. B. Mackenzie, *On the Elimination of Scale Ambiguities in Perturbative Quantum Chromodynamics*, *Phys. Rev. D* **28** (1983) 228.
- [101] A. H. Hoang and I. W. Stewart, *Designing gapped soft functions for jet production*, *Phys. Lett. B* **660** (2008) 483 [[0709.3519](#)].
- [102] M. Kologlu, P. Kravchuk, D. Simmons-Duffin and A. Zhiboedov, *The light-ray ope and conformal colliders*, *Journal of High Energy Physics* **2021** (2021) 1.
- [103] E. Gardi and J. Rathsmann, *Renormalon resummation and exponentiation of soft and collinear gluon radiation in the thrust distribution*, *Nucl. Phys. B* **609** (2001) 123 [[hep-ph/0103217](#)].
- [104] A. H. Hoang and S. Kluth, *Hemisphere Soft Function at $O(\alpha_s^2)$ for Dijet Production in e^+e^- Annihilation*, [0806.3852](#).
- [105] R. Brüser, Z. L. Liu and M. Stahlhofen, *Three-Loop Quark Jet Function*, *Phys. Rev. Lett.* **121** (2018) 072003 [[1804.09722](#)].
- [106] A. H. Hoang, A. Jain, C. Lepenik, V. Mateu, M. Preisser, I. Scimemi et al., *The MSR mass and the $\mathcal{O}(\Lambda_{\text{QCD}})$ renormalon sum rule*, *JHEP* **04** (2018) 003 [[1704.01580](#)].
- [107] K. G. Chetyrkin, J. H. Kuhn and A. Kwiatkowski, *QCD corrections to the e^+e^- cross-section and the Z boson decay rate*, *Phys. Rept.* **277** (1996) 189 [[hep-ph/9503396](#)].